

Nonclassical characteristics in spin-1/2 Heisenberg XYZ model with added DM and KSEA interactions under sinusoidal magnetic field: Hierarchy of quantum resources

A. Ali^{1,*}, S. Al-Kuwari¹, M. T. Rahim¹, M. Ghominejad², H. Ali³ and S. Haddadi^{2,†}

¹*Qatar Centre for Quantum Computing (QC2), College of Science and Engineering, Hamad Bin Khalifa University, Qatar Foundation, Doha, Qatar*

²*Faculty of Physics, Semnan University, P.O. Box 35195-363, Semnan, Iran*

³*Department of Physics, Abbottabad University of Science and Technology, P.O. Box 22500 Havelian KP, Pakistan*

(Dated: May 28, 2024)

We investigate the behavior of various measures of quantum coherence and quantum correlation in the spin-1/2 Heisenberg XYZ model with added Dzyaloshinsky-Moriya (DM) and Kaplan-Shekhtman-Entin-Wohlmman-Aharony (KSEA) interactions at a thermal regime described by a Gibbs density operator. We aim to understand the restricted hierarchical classification of different quantum resources, where quantum coherence \supseteq quantum discord \supseteq quantum entanglement \supseteq quantum steering \supseteq Bell nonlocality. In order to enhance quantum coherence, quantum correlation, and fidelity of teleportation, our analysis encompasses the effects of independently provided sinusoidal magnetic field control as well as DM and KSEA interactions on the considered system. The results reveal that enhancing the entanglement or quantum correlation of the channel does not always guarantee successful teleportation or even an improvement in teleportation fidelity. Thus, the relationship between teleportation fidelity and the channel's underlying quantum properties is intricate. Our study provides valuable insights into the complex interplay of quantum coherence and correlation hierarchy, offering potential applications for quantum communication and information processing technologies.

Keywords: Heisenberg XYZ model, quantum coherence, quantum correlation, teleportation

I. INTRODUCTION

Quantum coherence is a broad concept that encompasses all kinds of quantum correlations within a multipartite quantum system [1, 2]. When the off-diagonal elements of a density matrix are non-zero, it indicates the presence of quantum coherence. Baumgratz *et al.* [2] introduced a quantum resource theory of quantum coherence, where the l_1 -norm of coherence effectively quantifies this notion. This quantum coherence can stem from all forms of separable and non-separable correlations, such as nonlocality, quantum steering (QS), entanglement, and quantum discord (QD)[3–7]. Figure 1 illustrates the hierarchy of quantum correlations, where each layer represents a subset of the one encompassing it, with quantum coherence being the largest and most inclusive, and nonlocality being the most specific and restrictive. This hierarchical structure visually represents how each type of quantum correlations may build upon the previous ones, showcasing their interrelations and dependencies [8–10].

Entanglement refers to the remarkable nonseparable quantum correlations between particles, where the state of one particle instantaneously influences the state of another, regardless of distance. QD extends beyond entanglement, encompassing all quantum correlations residing in both separable and nonseparable states shared between subsystems of a quantum system [5–7]. For pure

nonseparable states, QD and entanglement are equivalent [6, 7], but this is not the case for mixed states.

QS [11–14] represents a unique form of quantum correlations. In a scenario where two distant observers share an entangled quantum state, QS describes the ability of one observer to remotely influence the state of the other observer's system. While entanglement entails quantum correlations between quantum particles regardless of distance, QS introduces an asymmetry in the observer's roles. In a QS scenario, one observer can manipulate the state of the other observer's system, but the reverse may not always hold. This fundamental asymmetry sets QS apart and raises intriguing questions about the relationship between QS, entanglement, and nonlocality. However, the quantum correlation measures discussed above are highly complex and intricately linked, making it challenging to definitively distinguish between them, even in the context of two- and three-qubit systems. In essence, these measures exhibit intricate interconnections, reflecting the nuanced nature of quantum correlations.

Nonlocality is a concept that arises from the violation of certain inequalities known as Bell inequalities [15, 16]. These inequalities describe limits on quantum correlations that can occur between distant systems within a classical framework. When these inequalities are violated, it implies that the quantum correlations between the systems cannot be explained by local hidden variables (underlying properties or information that determine the outcome of measurements) and suggests a form of nonlocality in quantum mechanics. From Bell inequalities, we now understand that entanglement and nonlocality are synonymous in a pure state, meaning that entanglement implies nonlocality and vice versa. However, the situ-

* asal68826@hbku.edu.qa

† haddadi@semnan.ac.ir

ation is not clear and simple for mixed states, even in two-qubit systems[17–20].

A one-dimensional Heisenberg spin chain is a theoretical model generally used in condensed matter physics to describe a linear array of interacting quantum spins [21–28]. Each spin interacts with its nearest neighbors, exhibiting phenomena such as quantum phase transitions and quantum correlations. In quantum technologies, Heisenberg spin chains offer potential for quantum simulation [29, 30], computing [31, 32], metrology and sensing [33–35], and communication [36, 37]. Entanglement properties of spin chains can be harnessed for quantum communication protocols, where one can use spin chains as quantum channels to transfer quantum states between distant parties securely and with higher fidelity compared to classical communication channels [38].

In this work, we take the most general two-qubit Heisenberg XYZ model under a sinusoidally controlled magnetic field applied to an individual spin site with asymmetric spin-orbit coupling interaction called Dzyaloshinsky-Moriya (DM) interaction and symmetric exchange coupling known as Kaplan–Shekhtman–Entin–Wohlmman–Aharony (KSEA) interaction, and study the behavior of all the aforementioned quantifiers with changes in the model parameters.

To elucidate the occurrence of weak ferromagnetism observed in certain rhombohedral antiferromagnets, Dzyaloshinsky [39–41] developed a phenomenological approach grounded in the Landau theory of second-order phase transitions. This approach highlighted that the appearance of a nonzero net magnetization in the system is attributed to the antisymmetric mixed term in the expansion of the thermodynamic potential. Additionally, Dzyaloshinsky noticed that in antiferromagnetic crystals with tetragonal lattices, weak ferromagnetism can be induced by the symmetric mixed term in the corresponding thermodynamic potential. In 1960, Moriya [42] improved the understanding by formulating a microscopic theory of anisotropic superexchange interaction, extending the Anderson theory of superexchange to include spin-orbit coupling. Through perturbation theory, Moriya identified the primary anisotropy contribution to the interaction between neighboring spins as the DM interaction. Moriya also revealed a second-order correction term involving a symmetric traceless tensor. While historically considered negligible, Kaplan and subsequently Shekhtman *et al.* [42–44] argued for the significance of the symmetric term. This term, called KSEA interaction as mentioned before, can restore the $O(3)$ invariance of the isotropic Heisenberg system, a property disrupted by the DM term. This reevaluation of the interaction emphasizes its importance in understanding weak ferromagnetism in antiferromagnetic systems.

Finally, we also consider a teleportation protocol by employing the two-qubit Heisenberg spin chain as a channel to study how the channel parameters can impact the fidelity of the teleported state. Heisenberg XYZ model has already been experimentally studied, such

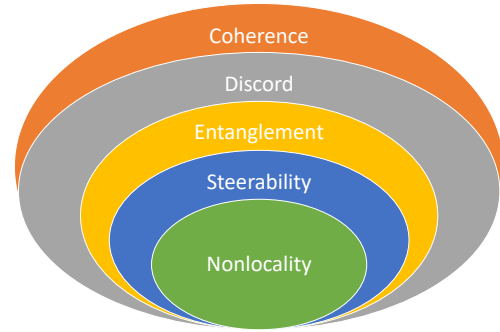


FIG. 1. Conventional hierarchy breakdown of quantum coherence and correlations, i.e. quantum coherence \supseteq QD \supseteq entanglement \supseteq QS \supseteq nonlocality.

as in Rydberg or dipolar atoms, through a combination of dipole interactions with engineered optical pumping [45]. Floquet-engineered XXZ spin coupling in bulk systems and optical tweezer arrays have been demonstrated in [46, 47]. Similarly, this model has been recently realized in multiple experiments, notably in dipolar-octupolar (DO) Kramers compounds $Ce_2(Sn, Zr)_2O_7$ and $Nd_2Zr_2O_7$ [48–50]. Moreover, the XYZ model has been realized in Weyl-Heisenberg ferromagnets [51].

A. Contribution

The contribution of this work is to explore the hierarchical classification of different quantum resources and their impact on teleportation fidelity. We analyze how magnetic field control as well as DM and KSEA interactions affect quantum coherence, correlations, and teleportation, revealing the nuanced relationship between teleportation fidelity and the channel's quantum properties. The work sheds light on the robustness of quantum resources under temperature variations and control parameters, offering crucial insights for developing quantum communication and information processing technologies.

B. Organization

The scheme of this paper is as follows: in Sec. II, we define and explain the different notions of quantum coherence and quantum correlation measures. In Sec. III, we briefly introduce the spin-1/2 Heisenberg XYZ model, diagonalize the system, and come up with the thermal state of the model. In Sec. IV, we present a simple teleportation scheme based on the considered model to be implemented. Section V presents the results and discussion, and finally, Sec. VI concludes this paper.

II. QUANTUM RESOURCES

A. l_1 -norm quantum coherence

Quantum coherence is a fundamental concept that arises from the superposition principle in quantum mechanics. A rigorous framework to quantify coherence as a resource, known as the resource theory of quantum coherence, has been previously developed [1, 2]. This theory identifies the set of incoherent states \mathcal{I} which are diagonal in a reference basis $\{|i\rangle\}$:

$$\delta \in \mathcal{I} \iff \delta = \sum_i \delta_i |i\rangle\langle i|. \quad (1)$$

The free operations are the incoherent operations that map incoherent states to incoherent states. Revealing and quantifying quantum coherence is essential to enable quantum correlations and information processing.

Accordingly, Baumgratz *et al.* [2] proposed the l_1 -norm of quantum coherence as a quantifier of coherence, given by

$$Q(\rho) = \sum_{i \neq j} |\langle i | \rho | j \rangle| = \sum_{i,j} |\rho_{ij}| - \sum_i |\rho_{ii}|, \quad (2)$$

where ρ is the density operator of the considered system.

B. Quantum discord

QD measures nonclassical correlations between subsystems in a quantum system, capturing quantumness not explained by classical means. QD quantifies differences between quantum and classical mutual information.

QD indicates the difference between total and classical correlation for a two-qubit system [5–7, 52]. That is, QD for a bipartite quantum X state, ρ_X is expressed as

$$D(\rho_X) = \min\{q_1, q_2\}, \quad (3)$$

where

$$q_j = H(\rho_{11} + \rho_{33}) + \sum_{i=1}^4 \lambda_i \log_2 \lambda_i + w_j, \quad (4)$$

here, λ_i 's represent the eigenvalues of density matrix ρ_X , and

$$w_1 = H(\xi), \quad (5)$$

$$w_2 = - \sum_i \rho_{ii} \log_2 \rho_{ii} - H(\rho_{11} + \rho_{33}), \quad (6)$$

with

$$H(\xi) = -\xi \log_2 \xi - (1 - \xi) \log_2 (1 - \xi), \quad (7)$$

and

$$\xi = \frac{1}{2} \left\{ 1 + \sqrt{[1 - 2(\rho_{33} + \rho_{44})]^2 + 4(|\rho_{14}| + |\rho_{23}|)^2} \right\}. \quad (8)$$

C. Concurrence

Concurrence is an entanglement monotone used to quantify the degree of entanglement in arbitrary two-qubit states [4, 53]. For a given density matrix ρ , concurrence $C(\rho)$ of two qubits is defined as follows

$$C(\rho) = \max\{0, \lambda_1 - \lambda_2 - \lambda_3 - \lambda_4\}. \quad (9)$$

where λ_i 's are the square roots of the eigenvalues of the matrix (non-Hermitian) $\rho(\sigma_y \otimes \sigma_y) \rho^* (\sigma_y \otimes \sigma_y)$ in decreasing order. As before, σ_y represents the y -component of Pauli matrices, and ρ^* denotes the complex conjugate of ρ . Note that the measure (9) takes values between 0 and 1, indicating the absence of entanglement when $C(\rho) = 0$ and maximal entanglement when $C(\rho) = 1$.

D. Quantum steering

Erwin Schrödinger proposed steering as an extension of the Einstein-Podolsky-Rosen paradox [11]. Though initially overlooked as nonlocal correlations, it later sparked significant advancements. Steerable states exhibit quantum advantages in device-independent quantum cryptography [54], secure teleportation [55], randomness generation [56], and subchannel discrimination [57]. The three-setting linear steering inequality [58, 59] is based on the assumption that either Alice or Bob are allowed three measurement observables on their respective subsystems. It is a crucial tool for detecting and quantifying steering in a state, particularly in a two-qubit system which reads

$$\frac{1}{\sqrt{3}} \sum_{i=1}^3 \text{Tr}(A_i \otimes B_i \rho) \leq 1, \quad (10)$$

where $A_i = a_i \cdot \sigma$ and $B_i = b_i \cdot \sigma$ are Hermitian operators acting on qubits A and B , respectively. Here, $a_i, b_i \in \mathbb{R}^3$ are two unit vectors with $\{b_1, b_2, b_3\}$ being orthogonal to each other, and Pauli matrices $\sigma = (\sigma_1 = \sigma_x, \sigma_2 = \sigma_y, \sigma_3 = \sigma_z)$. Any violation of the inequality (10) implies that ρ is steerable, and the maximal violation gives a measure of steering [59]. Explicitly,

$$S(\rho) = \max_{\{A_i, B_i\}} \left\{ \frac{1}{\sqrt{3}} \sum_{i=1}^3 \text{Tr}(A_i \otimes B_i \rho) \right\} \quad (11)$$

represents the maximum violation of the three-setting linear steering inequality.

E. Bell nonlocality

In order to quantify the degree of quantum nonlocality and enable a more thorough comparison of quantum correlations, one can use the Bell inequality violation.

The normalized form of Bell nonlocality function can be written as [60–64]

$$\mathcal{B}(\rho) = \max \left\{ 0, \frac{\mathcal{B}_{\text{CHSH}} - 2}{\mathcal{B}_{\text{max}} - 2} \right\}, \quad (12)$$

where $0 \leq \mathcal{B}(\rho) \leq 1$ since $\mathcal{B}_{\text{CHSH}} \leq \mathcal{B}_{\text{max}} = 2\sqrt{2}$ for a two-qubit system ρ . Notice, $\mathcal{B}_{\text{CHSH}}$ is the maximum violation of Bell Clauser–Horne–Shimony–Holt (CHSH) inequality.

III. HEISENBERG XYZ MODEL

The Hamiltonian describing a general Heisenberg XYZ model under the influence of an inhomogeneous magnetic field, including DM and KSEA interactions, is given by

$$\hat{\mathcal{H}}_N = \hat{\mathcal{H}}_H + \hat{\mathcal{H}}_B + \hat{\mathcal{H}}_{\text{DM}} + \hat{\mathcal{H}}_{\text{KSEA}}, \quad (13)$$

The initial term $\hat{\mathcal{H}}_H$ accounts for Heisenberg spin exchange interactions, with $\hat{\mathcal{H}}_B$ as the Zeeman Hamiltonian representing the influence of the inhomogeneous external magnetic field on the system. Additionally, $\hat{\mathcal{H}}_{\text{DM}}$ and $\hat{\mathcal{H}}_{\text{KSEA}}$ represent the DM interaction and KSEA interaction, respectively. This total Hamiltonian (13) can be explicitly written as [65, 66]

$$\begin{aligned} \hat{\mathcal{H}}_N = \sum_{i=1}^{N-1} & \{ J_x \hat{\sigma}_i^x \otimes \hat{\sigma}_{i+1}^x + J_y \hat{\sigma}_i^y \otimes \hat{\sigma}_{i+1}^y + J_z \hat{\sigma}_i^z \otimes \hat{\sigma}_{i+1}^z \\ & + \vec{\mathcal{B}}_i \cdot (\vec{\sigma}_i \otimes \mathbb{I}_2) + \vec{\mathcal{B}}_{i+1} \cdot (\mathbb{I}_2 \otimes \vec{\sigma}_{i+1}) \\ & + \vec{\mathcal{D}} \cdot (\vec{\sigma}_i \times \vec{\sigma}_{i+1}) + \vec{\sigma}_i \cdot \Gamma \cdot \vec{\sigma}_{i+1} \}, \end{aligned} \quad (14)$$

here,

$$\Gamma = \begin{pmatrix} 0 & \Gamma_z & \Gamma_y \\ \Gamma_z & 0 & \Gamma_x \\ \Gamma_y & \Gamma_x & 0 \end{pmatrix}. \quad (15)$$

$$\hat{\mathcal{H}} = \begin{pmatrix} J_z + B(\cos \theta + \sin \theta) & 0 & 0 & -2i\Gamma_z + J_x - J_y \\ 0 & -J_z + B(\cos \theta - \sin \theta) & -2iD_z + J_x + J_y & 0 \\ 0 & -2iD_z + J_x + J_y & -J_z - B(\cos \theta - \sin \theta) & 0 \\ 2i\Gamma_z + J_x - J_y & 0 & 0 & J_z - B(\cos \theta + \sin \theta) \end{pmatrix}. \quad (17)$$

The diagonalization of $\hat{\mathcal{H}}$ (17) results in four eigenvalues, given by

$$\begin{aligned} E_{1,2} &= \pm \mathcal{K}_1 + J_z, \\ E_{3,4} &= \pm \mathcal{K}_2 - J_z, \end{aligned} \quad (18)$$

with expressions

$$\mathcal{K}_1 = \sqrt{k_1^2 + B^2 (\cos \theta + \sin \theta)^2}$$

The interaction between neighboring spin sites is determined by the real spin–spin coupling coefficients along the x , y , and z directions, denoted as J_k for $k = x, y, z$. Antiferromagnetic coupling is indicated by positive values of J_k , while negative values represent ferromagnetic coupling. The standard Pauli spin operators, denoted as $\hat{\sigma}_i^k$, define the spin vector on the i th site as $\vec{\sigma}_i = (\hat{\sigma}_i^x, \hat{\sigma}_i^y, \hat{\sigma}_i^z)$. Moreover, $\vec{\mathcal{B}}_i = (B_i^x, B_i^y, B_i^z)$ represents the magnetic flux density contributing to Zeeman splitting at the i th spin site. The DM interaction vector is defined by $\vec{\mathcal{D}} = (D_x, D_y, D_z)$ and serves as the anti-symmetric exchange coupling responsible for spin–orbit coupling in specific materials. Note that the KSEA interaction (Γ) introduces an anisotropic symmetric interaction [65–68].

Given the complexity of the model involving numerous parameters, we find it cumbersome to maintain full generality. Instead, we simplify the scenario by focusing on a situation involving two adjacent spin sites. In this context, let $\vec{\mathcal{B}}_1 = (0, 0, B \cos \theta)$, $\vec{\mathcal{B}}_2 = (0, 0, B \sin \theta)$, $\vec{\mathcal{D}} = (0, 0, D_z)$, and specify that $\Gamma_x = \Gamma_y = 0$ while $\Gamma_z \neq 0$. Consequently, our Hamiltonian (14) can be expressed in a modified form applicable to any pair of consecutive spin sites as

$$\begin{aligned} \hat{\mathcal{H}} = & J_x \hat{\sigma}_1^x \otimes \hat{\sigma}_2^x + J_y \hat{\sigma}_1^y \otimes \hat{\sigma}_2^y + J_z \hat{\sigma}_1^z \otimes \hat{\sigma}_2^z \\ & + B [\cos \theta (\hat{\sigma}_1^z \otimes \mathbb{I}_2) + \sin \theta (\mathbb{I}_2 \otimes \hat{\sigma}_2^z)] \\ & + D_z (\hat{\sigma}_1^x \otimes \hat{\sigma}_2^y - \hat{\sigma}_1^y \otimes \hat{\sigma}_2^x) \\ & + \Gamma_z (\hat{\sigma}_1^x \otimes \hat{\sigma}_2^y + \hat{\sigma}_1^y \otimes \hat{\sigma}_2^x). \end{aligned} \quad (16)$$

As we know, this Hamiltonian (16) has a standard X-structured matrix form. Using the standard computational basis $\{|00\rangle, |01\rangle, |10\rangle, |11\rangle\}$, it can be expressed in a simplified form

and

$$\mathcal{K}_2 = \sqrt{k_2^2 + B^2 (\cos \theta - \sin \theta)^2},$$

where

$$k_1 = \sqrt{(J_x - J_y)^2 + 4\Gamma_z^2}$$

and

$$k_2 = \sqrt{(J_x + J_y)^2 + 4D_z^2}.$$

The state of a system in the thermal equilibrium with the absolute temperature T is described by the Gibbs density operator

$$\rho_T = \frac{1}{Z} e^{-\hat{\mathcal{H}}/\kappa_B T}, \quad (19)$$

where $Z = \text{Tr}[\exp(-\hat{\mathcal{H}}/\kappa_B T)]$ is partition function with the Boltzmann constant κ_B (considered as $\kappa_B = 1$ for simplification purpose).

Using now Hamiltonian (17) and density operator (19), we obtain the following density matrix at thermal equilibrium

$$\rho_T = \begin{pmatrix} a^- & 0 & 0 & c \\ 0 & b^- & d & 0 \\ 0 & d^* & b^+ & 0 \\ c^* & 0 & 0 & a^+ \end{pmatrix}, \quad (20)$$

where the nonzero elements read

$$\begin{aligned} a^\pm &= \frac{e^{-J_z/T}}{Z} \{ \cosh(\mathcal{K}_1/T) \pm [B(\cos\theta + \sin\theta)/\mathcal{K}_1] \Theta_1 \}, \\ b^\pm &= \frac{e^{J_z/T}}{Z} \{ \cosh(\mathcal{K}_2/T) \pm [B(\cos\theta - \sin\theta)/\mathcal{K}_2] \Theta_2 \}, \\ c &= -\frac{e^{-J_z/T}}{Z} [(-2i\Gamma_z + J_x - J_y)/\mathcal{K}_1] \Theta_1, \\ d &= -\frac{e^{J_z/T}}{Z} [(2iD_z + J_x + J_y)/\mathcal{K}_2] \Theta_2, \end{aligned} \quad (21)$$

where $\Theta_{(1)2} = \sinh(\mathcal{K}_{(1)2}/T)$, and

$$Z = 2 \left[e^{-J_z/T} \cosh(\mathcal{K}_1/T) + e^{J_z/T} \cosh(\mathcal{K}_2/T) \right], \quad (22)$$

The state presented in Eq. (20) has an X structure. Thus, the explicit expressions of the aforementioned quantifiers based on thermal state elements (21) can be derived straightforwardly.

For example, the l_1 -norm of quantum coherence (2) can be obtained as

$$Q(\rho_T) = |c| + |c^*| + |d| + |d^*|. \quad (23)$$

Moreover, the analytical expression of QD for our thermal state (20) would be given by Eq. (3) with considering $\rho_{11} = a^-$, $\rho_{22} = b^-$, $\rho_{33} = b^+$, $\rho_{44} = a^+$, $\rho_{14} = c$, and $\rho_{23} = d$.

Regarding the analytical form of QS (11), one needs to simply obtain $\text{Tr}(A_i \otimes B_i \rho_T)$. Explicitly, we have

$$\begin{aligned} S(\rho_T) &= \{8(cc^* + dd^*) - 4a^-(b^- + b^+) \\ &\quad - 4a^+(b^- - b^+) + 1\}^{1/2}. \end{aligned} \quad (24)$$

Besides, the concurrence (9) can be derived as

$$C(\rho_T) = 2 \max \{0, t_1, t_2\}, \quad (25)$$

$$\text{where } t_1 = |d| - \sqrt{a^- a^+} \text{ and } t_2 = |c| - \sqrt{b^- b^+}.$$

Finally, the normalized form of Bell nonlocality function (12) is found to be

$$\mathcal{B}(\rho_T) = \max \left\{ 0, (2 \max\{0, m_1, m_2\} - 2)/(2\sqrt{2} - 2) \right\}, \quad (26)$$

$$\text{where } m_1 = \sqrt{4(|c| + |d|)^2 + (a^- - b^- - b^+ + a^+)^2} \text{ and } m_2 = \sqrt{8(|c|^2 + |d|^2)}.$$

IV. QUANTUM TELEPORTATION

In this section, we examine the teleportation protocol, considering ρ_T as the quantum channel state, assuming the input state is an arbitrary unknown pure state consisting of two qubits such as

$$|\psi_{\text{in}}\rangle = \cos(\alpha/2)|10\rangle + e^{i\phi} \sin(\alpha/2)|01\rangle, \quad (27)$$

where α and ϕ represent the amplitude and phase of the target state to be teleported, respectively. The quantum channel is known as a completely positive and trace-preserving operator. Through this process, an input state is mapped to an output state.

When a quantum state is teleported via the mixed channel ρ_{ch} , the resulting output replica state ρ_{out} is achieved by performing joint measurements and local unitary transformations on the input state $\rho_{\text{in}} = |\psi_{\text{in}}\rangle\langle\psi_{\text{in}}|$

$$\rho_{\text{out}} = \sum_{i,j \in \{0,x,y,z\}} p_i p_j (\sigma^i \otimes \sigma^j) \rho_{\text{in}} (\sigma^i \otimes \sigma^j), \quad (28)$$

where $\sigma^0 = \mathbb{I}_2$, and $p_i = \text{Tr}(q^i \rho_{\text{ch}})$ satisfies the condition $\sum_i p_i = 1$. Moreover, we have $q^0 = |\Psi^-\rangle\langle\Psi^-|$, $q^1 = |\Phi^-\rangle\langle\Phi^-|$, $q^2 = |\Psi^+\rangle\langle\Psi^+|$, and $q^3 = |\Phi^+\rangle\langle\Phi^+|$ in which $|\Psi^\pm\rangle$ and $|\Phi^\pm\rangle$ are four Bell states. Here, let us suppose that the quantum channel is a thermal state (20), namely $\rho_{\text{ch}} = \rho_T$.

The quality of the teleported state is determined by the criterion of fidelity $F(\rho_{\text{in}}, \rho_{\text{out}})$, defined as

$$F(\rho_{\text{in}}, \rho_{\text{out}}) = \left(\text{Tr} \sqrt{\sqrt{\rho_{\text{in}}} \rho_{\text{out}} \sqrt{\rho_{\text{in}}}} \right)^2. \quad (29)$$

Based on the above definition, the average fidelity of teleportation \mathcal{F} is given by

$$\mathcal{F} = \frac{1}{4\pi} \int_0^{2\pi} d\phi \int_0^\pi d\alpha F(\rho_{\text{in}}, \rho_{\text{out}}) \sin \alpha. \quad (30)$$

The maximum classical average fidelity threshold is observed at $\mathcal{F} = 2/3$. Beyond this point, we transition

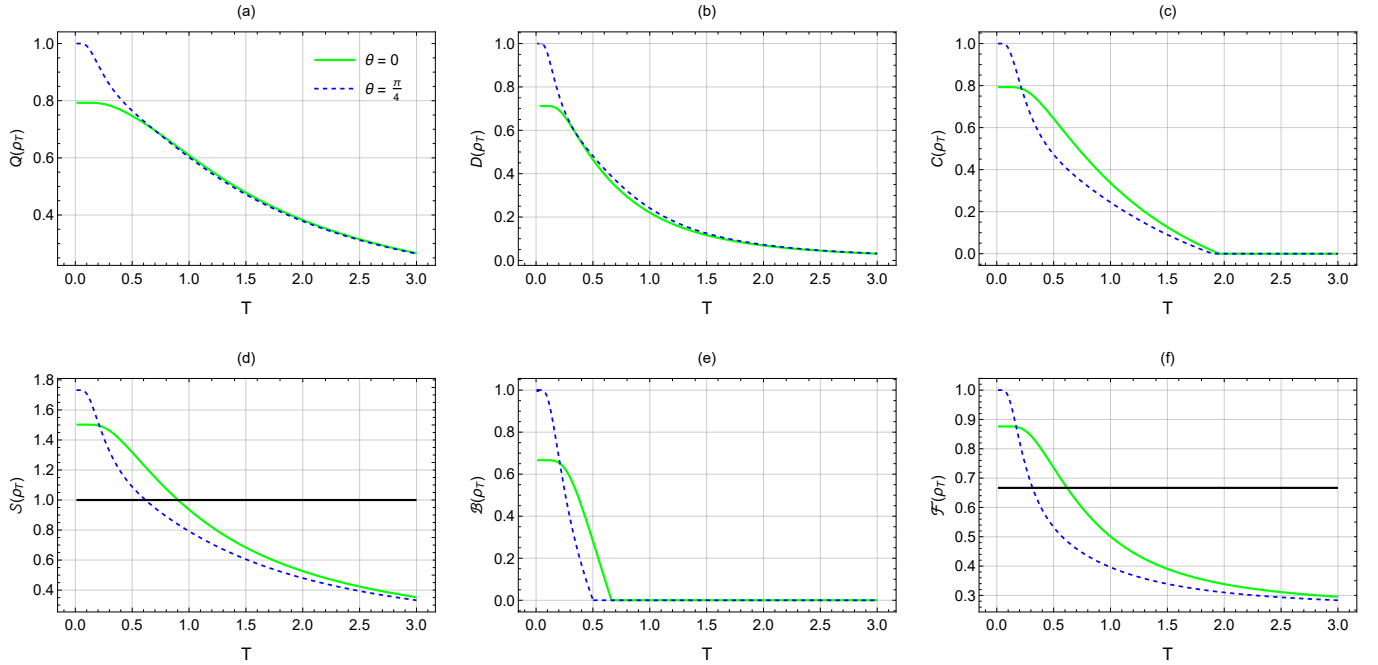


FIG. 2. The variations of l_1 -norm quantum coherence (a), QD (b), concurrence (c), QS (d), Bell nonlocality (e), and average fidelity (f) as a function of temperature T at $J_x = 0.8$, $J_y = 0.5$, $J_z = 0.3$, $D_z = 0$, $\Gamma_z = 0$ when the magnetic field is applied to single spin ($\theta = 0$), and when a same magnetic field is applied to both spins ($\theta = \pi/4$). Black horizontal lines show $S(\rho_T) = 1$ in (d) and $\mathcal{F}(\rho_T) = 2/3$ in (f).

into the quantum average fidelity regime. The proximity of the quantum average fidelity to unity signifies reduced information leakage, indicating optimal conditions for quantum teleportation.

In our case (density matrix (20)), the analytical form of average fidelity is derived by

$$\mathcal{F}(\rho_T) = \frac{2}{3}(b^- + b^+)^2 + \frac{1}{3}(a^- + a^+)^2 + \frac{1}{3}(d + d^*)^2. \quad (31)$$

V. RESULTS AND DISCUSSION

In this investigation, our objective is to analyze various quantum coherence and correlation measures within the Heisenberg XYZ model, using it as a quantum resource channel for teleporting a target quantum state $|\psi_{\text{in}}\rangle = \cos(\alpha/2)|10\rangle + e^{i\phi}\sin(\alpha/2)|01\rangle$. The goal is to enhance average quantum teleportation fidelity beyond $2/3$ by adjusting parameters such as magnetic field, bath temperature, and DM and KSEA interactions, thereby enhancing the channel's quantum resources. We consider an antiferromagnetic spin chain characterized by anisotropic spin–spin coupling constants (a random case): $J_x = 0.8$, $J_y = 0.5$, and $J_z = 0.3$.

A. Impact of Magnetic Field

First, our focus is on the impact of applying a magnetic field to either one spin ($\theta = 0$ or $\theta = \pi/2$) or to both spins ($\theta = \pi/4$) with $B = 1$ on quantum resources and teleportation fidelity in the absence of DM and KSEA interactions. Figure 2 illustrates the variations of quantum resources and teleportation fidelity with temperature under zero DM and KSEA interactions, comparing two distinct fixed magnetic field values.

In Figs. 2(a) and 2(b), the l_1 norm of quantum coherence and quantum discord are shown as functions of temperature. At low temperatures, peak values are higher when the same magnetic field is applied to both spins (dashed blue curve) compared to when it is applied to just one spin (solid green curve). Both measures decrease with increasing temperature. This result does not surprise us because the temperature can diminish the quantum coherence and correlation due to thermal fluctuations in the system.

Figures 2(c), 2(d), and 2(e) depict the behaviors of concurrence, QS, and Bell nonlocality versus T , respectively. The entanglement captured by concurrence disappears after $T \approx 1.9$. Note that at low temperatures, peak values of concurrence are greater when the same magnetic field is applied to both spins (dashed blue curve). Our findings show that for $0.7 \leq T \leq 0.9$, the channel state is steerable without nonlocality, as $S(\rho_T) > 1$ in Fig. 2(d). Between $T \approx 0.7$ and $T \approx 1.9$, the channel state

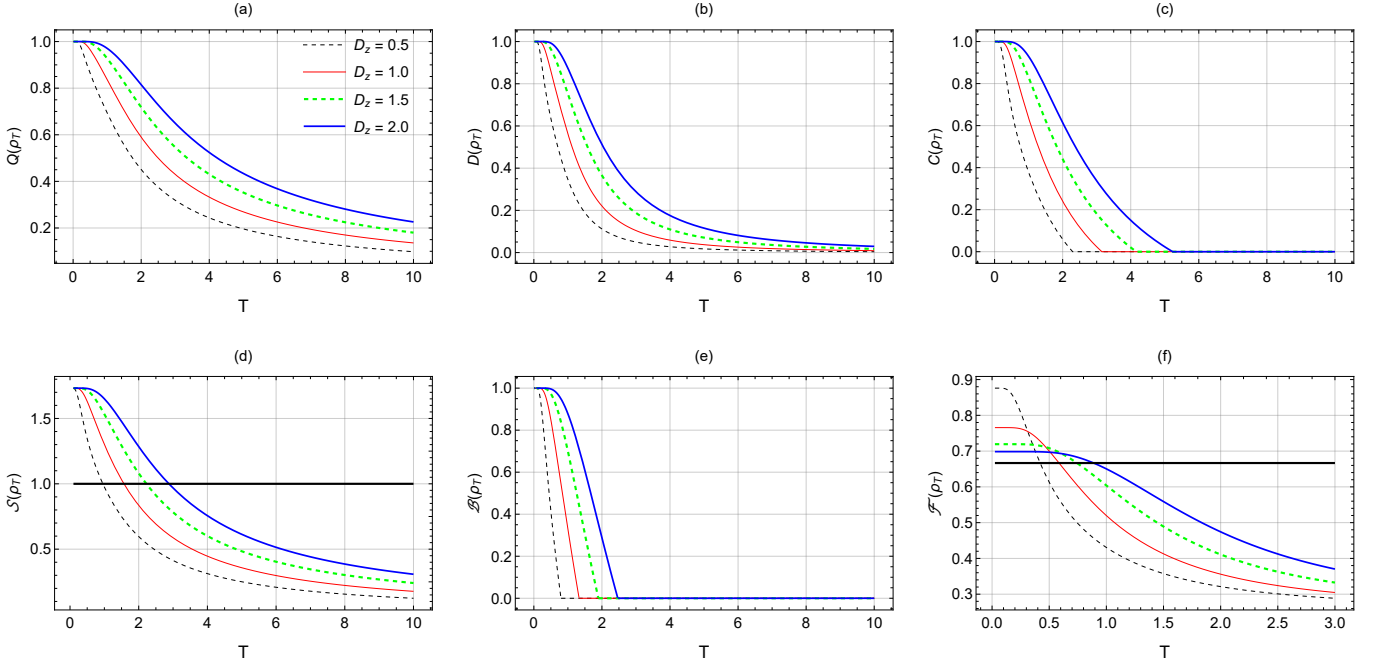


FIG. 3. The behaviors of l_1 -norm quantum coherence (a), QD (b), concurrence (c), QS (d), Bell nonlocality (e), and average fidelity (f) versus temperature T at $J_x = 0.8$, $J_y = 0.5$, $J_z = 0.3$, $\theta = \pi/4$, and $\Gamma_z = 0$ for different fixed values of D_z .

remains entangled [see Fig. 2(c)] but without nonlocality [see Fig. 2(e)]. More precisely, Bell nonlocality decreases to zero before concurrence and discord as the channel becomes thermally mixed. Notice, $Q(\rho_T)$ and $D(\rho_T)$ show more robustness compared to $C(\rho_T)$, $S(\rho_T)$, and $B(\rho_T)$. Thus, the mixed entangled states can exist without violating Bell inequalities or exhibiting nonlocality. These highlight the hierarchical relationship between the mentioned quantum resources.

Our results in Fig. 2 indicate that applying the same magnetic field to both qubits significantly enhances average teleportation fidelity [see Fig. 2(f)], quantum coherence, and correlations at low temperatures. These enhancements diminish at higher temperatures due to thermal effects. However, fidelity remains above the classical limit $\mathcal{F}(\rho_T) = 2/3$ at low temperatures for both $\theta = 0$ and $\theta = \pi/4$, with maximum fidelity achieved for $\theta = \pi/4$.

From Fig. 2, we conclude that applying the same magnetic field to both qubits enhances teleportation fidelity and quantum correlations more significantly across different temperatures compared to applying it to just one qubit. The hierarchy of quantum resources—quantum coherence \supseteq QD \supseteq entanglement \supseteq QS \supseteq nonlocality—depicted in Figs. 1 and 2, demonstrates that the Bell nonlocality function is the weakest measure, while the l_1 -norm of coherence is the strongest indicator of non-classical characteristics.

Given that using the same magnetic field control for both spins enhances quantum coherence and correlations as well as average teleportation fidelity at low tempera-

tures, we will adopt $\theta = \pi/4$ as the standard setting and explore other model parameters to improve these measures against the increasing of temperature.

B. Impact of DM Interaction

Next, we examine the impact of different fixed values of DM interaction, without introducing KSEA interaction, on the quantum resources and the average fidelity of teleportation. This analysis is presented in Fig. 3 where the considered functions are evaluated against temperature T for various fixed values of DM interaction: $D_z = 0.5$ (dashed black), $D_z = 1.0$ (solid red), $D_z = 1.5$ (dashed green), and $D_z = 2.0$ (solid blue).

We observe that although DM interaction does not increase the peak values of these functions, it aids in maintaining high peak values of quantum resources even at significantly higher temperatures (compare with Fig 2 when $D_z = 0$). Thus, we can consider its effect as a positive influence on all quantum coherence and correlations of the quantum channel. For instance, when $D_z = 0.5$, Bell nonlocality diminishes to zero around $T \approx 0.9$, whereas for $D_z = 2.0$, it decreases to zero at $T \approx 2.5$, marking more than a five-fold improvement in the sustainability of Bell nonlocality. A similar trend is observed for QD and concurrence, with even higher T values. Notably, among all quantum resources, Bell nonlocality is the most delicate, followed by QS.

Despite achieving maximal entanglement at near-zero temperatures, the average teleportation fidelity remains

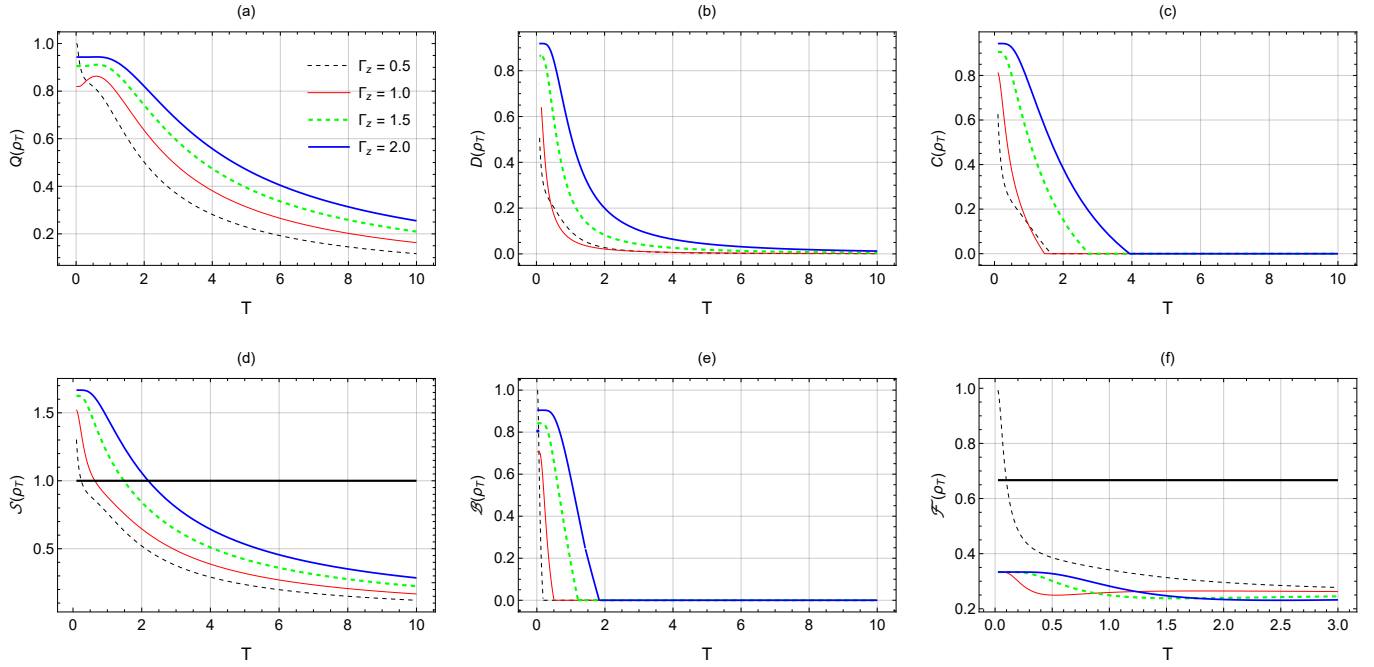


FIG. 4. The behaviors of l_1 -norm quantum coherence (a), QD (b), concurrence (c), QS (d), Bell nonlocality (e), and average fidelity (f) versus temperature T at $J_x = 0.8$, $J_y = 0.5$, $J_z = 0.3$, $\theta = \pi/4$, and $D_z = 0$ for different fixed values of Γ_z .

greater than the classical limit of $2/3$, indicating successful but not maximal teleportation. At low temperatures, the value of teleportation fidelity slightly decreases with larger DM interactions. However, this underscores that the maximal entanglement in a mixed-state situation does not always guarantee ideally successful teleportation, even at the lowest T values. Thus, increasing the DM interaction decreases the peak value of the average fidelity of teleportation while making it stable at higher temperatures. Nevertheless, this shows that maintaining the nonclassical characteristics at higher temperatures with increased DM interaction does not guarantee enhanced values of average teleportation fidelity.

In summary, increasing DM interaction generally enhances all the quantum correlations and coherence in our work but does not significantly increase the peak value of average teleportation fidelity, although it helps maintain these values at higher T . Again, the hierarchy of quantum resources, as depicted in Fig. 1, is held.

C. Impact of KSEA Interaction

Finally, we explore the impact of various fixed values of KSEA interaction, without introducing DM interaction, on quantum resources and the average fidelity of teleportation. This analysis is illustrated in Fig. 4 when we have plotted all functions against T for different fixed values of KSEA interaction: $\Gamma_z = 0.5$ (dashed black), $\Gamma_z = 1.0$ (solid red), $\Gamma_z = 1.5$ (dashed green), and $\Gamma_z = 2.0$ (solid blue) with zero value of D_z . One can observe that, unlike

DM interaction, KSEA interaction increases the peak values of these measures [compare with Fig 3 when $\Gamma_z = 0$]. Besides, it helps to maintain high peak values of quantum coherence and quantum correlations even at significantly higher temperatures. In general, its effect is positive on all quantum resources of the quantum channel. For instance, when $\Gamma_z = 0.5$, Bell nonlocality diminishes to zero around $T \approx 0.2$, whereas for $\Gamma_z = 2.0$, it decreases to zero at $T \approx 1.8$, marking a more than nine-fold improvement in the sustainability of Bell nonlocality. A similar trend is observed for QD and concurrence. Again, among all quantum resources, Bell nonlocality remains the most delicate, followed by QS.

Despite achieving maximal entanglement at very low temperatures, the average teleportation fidelity only remains greater than the classical limit ($2/3$) when KSEA interaction is very small [look at Fig. 4(f)]. Namely, at $\Gamma_z = 0.5$, the average fidelity of teleportation is greater than $2/3$ at near-zero temperatures, whereas increasing KSEA interaction does not help in achieving fidelity greater than $2/3$ even at low temperatures. This shows that increasing the KSEA interaction does not enhance teleportation fidelity and can not guarantee successful teleportation.

Although a large value of KSEA interaction does not enhance the average fidelity of teleportation, it is beneficial for enhancing quantum coherence and correlations (quantum resources). Therefore, increasing KSEA interaction enhances all the correlations and coherence but does not increase the peak value of average teleportation fidelity. While it helps maintain these values at higher T .

Overall, the impact of KSEA interaction on teleportation fidelity is negative.

Achieving a quantum advantage for teleportation is unsuccessful across all temperatures with different fixed KSEA interaction values. Although quantum coherence and correlations generally persist at nonzero levels for even higher temperatures, indicating the presence of nonlocality, entanglement, discord, and steering, successful quantum teleportation (greater than $\mathcal{F}(\rho_T) = 2/3$) is not achieved in this scenario. Additionally, we find that the channel state exhibits nonlocality and steerability, as well as entanglement, yet teleportation remains unachievable.

VI. CONCLUSION AND OUTLOOK

In this work, we investigate the behavior of various quantum resources in the spin-1/2 Heisenberg XYZ model with added Dzyaloshinsky-Moriya (DM) and Kaplan-Shekhtman-Entin-Wohlman-Aharony (KSEA) interactions under sinusoidal magnetic field. Our analysis has revealed the intricate interplay between the measures of nonclassical characteristics, shedding light on the restricted hierarchical classification of quantum resources: quantum coherence \supseteq quantum discord \supseteq entanglement \supseteq quantum steering \supseteq Bell nonlocality. Our results demonstrate that applying the same magnetic field to both qubits significantly enhances quantum coherence, correlations, and teleportation fidelity at low temperatures. However, increasing the DM interaction or KSEA interaction does not necessarily improve the peak telepor-

tation fidelity, despite enhancing and sustaining quantum resources at higher temperatures. We found that maximal entanglement does not guarantee optimal teleportation, even at the lowest temperatures, highlighting the complex relationship between teleportation fidelity and the underlying quantum properties of the channel. This study provides valuable insights into the nuanced interplay between quantum coherence, correlations, and their practical implications for quantum communication and information processing technologies. These findings underscore the importance of carefully considering and optimizing various quantum resources for specific applications, as enhancements in certain measures do not necessarily translate to improvements in others.

ACKNOWLEDGEMENTS

M.G. and S.H. were supported by Semnan University under Contract No. 21270.

DISCLOSURES

The authors declare that they have no known competing financial interests.

DATA AVAILABILITY

No datasets were generated or analyzed during the current study.

[1] A. Streltsov, G. Adesso, and M. B. Plenio, Colloquium: Quantum coherence as a resource, *Reviews of Modern Physics* **89**, 041003 (2017).

[2] T. Baumgratz, M. Cramer, and M. B. Plenio, Quantifying coherence, *Physical Review Letters* **113**, 140401 (2014).

[3] R. Horodecki, P. Horodecki, M. Horodecki, and K. Horodecki, Quantum entanglement, *Reviews of Modern Physics* **81**, 865 (2009).

[4] W. K. Wootters, Entanglement of formation of an arbitrary state of two qubits, *Physical Review Letters* **80**, 2245 (1998).

[5] H. Ollivier and W. H. Zurek, Quantum discord: a measure of the quantumness of correlations, *Physical Review Letters* **88**, 017901 (2001).

[6] S. Luo, Quantum discord for two-qubit systems, *Physical Review A* **77**, 042303 (2008).

[7] M. Ali, A. Rau, and G. Alber, Quantum discord for two-qubit X states, *Physical Review A* **81**, 042105 (2010).

[8] Z.-H. Ma, J. Cui, Z. Cao, S.-M. Fei, V. Vedral, T. Byrnes, and C. Radhakrishnan, Operational advantage of basis-independent quantum coherence, *Europhysics Letters* **125**, 50005 (2019).

[9] H. M. Wiseman, S. J. Jones, and A. C. Doherty, Steering, entanglement, nonlocality, and the Einstein-Podolsky-Rosen paradox, *Physical Review Letters* **98**, 140402 (2007).

[10] A. U. Rahman, M. Y. Abd-Rabbou, S. Haddadi, and H. Ali, Two-qubit steerability, nonlocality, and average steered coherence under classical dephasing channels, *Annalen der Physik* **535**, 2200523 (2023).

[11] E. Schrödinger, Discussion of probability relations between separated systems, in *Mathematical Proceedings of the Cambridge Philosophical Society*, Vol. 31 (Cambridge University Press, 1935) pp. 555–563.

[12] R. Uola, A. C. Costa, H. C. Nguyen, and O. Gühne, Quantum steering, *Reviews of Modern Physics* **92**, 015001 (2020).

[13] M.-M. Du and D. Tong, Relationship between first-order coherence and the maximum violation of the three-setting linear steering inequality for a two-qubit system, *Physical Review A* **103**, 032407 (2021).

[14] A.-S. F. Obada, M. Y. Abd-Rabbou, and S. Haddadi, Does conditional entropy squeezing indicate normalized entropic uncertainty relation steering?, *Quantum Information Processing* **23**, 90 (2024).

[15] N. Brunner, D. Cavalcanti, S. Pironio, V. Scarani, and S. Wehner, Bell nonlocality, *Reviews of Modern Physics* **86**, 419 (2014).

[16] M. T. Quintino, T. Vértesi, D. Cavalcanti, R. Augusiak, M. Demianowicz, A. Acín, and N. Brunner, Inequivalence of entanglement, steering, and Bell nonlocality for general measurements, *Physical Review A* **92**, 032107 (2015).

[17] C. H. Bennett, D. P. DiVincenzo, C. A. Fuchs, T. Mor, E. Rains, P. W. Shor, J. A. Smolin, and W. K. Wootters, Quantum nonlocality without entanglement, *Physical Review A* **59**, 1070 (1999).

[18] S. Halder, M. Banik, S. Agrawal, and S. Bandyopadhyay, Strong quantum nonlocality without entanglement, *Physical Review Letters* **122**, 040403 (2019).

[19] S. S. Bhattacharya, S. Saha, T. Guha, and M. Banik, Nonlocality without entanglement: Quantum theory and beyond, *Physical Review Research* **2**, 012068 (2020).

[20] J. Niset and N. J. Cerf, Multipartite nonlocality without entanglement in many dimensions, *Physical Review A* **74**, 052103 (2006).

[21] M. Mahmoudi, S. Mahdavifar, T. M. A. Zadeh, and M. Soltani, Non-Markovian dynamics in the extended cluster spin-1/2 XX chain, *Physical Review A* **95**, 012336 (2017).

[22] S. Yin, S. Liu, J. Song, and H. Luan, Markovian and non-markovian dynamics of quantum coherence in the extended XX chain, *Physical Review A* **106**, 032220 (2022).

[23] T. Werlang and G. Rigolin, Thermal and magnetic quantum discord in Heisenberg models, *Physical Review A* **81**, 044101 (2010).

[24] F. Pinheiro, G. M. Bruun, J.-P. Martikainen, and J. Larsson, XYZ quantum Heisenberg models with *p*-orbital bosons, *Physical Review Letters* **111**, 205302 (2013).

[25] M. Y. Abd-Rabbou, A. U. Rahman, M. A. Yurishev, and S. Haddadi, Comparative study of quantum Otto and Carnot engines powered by a spin working substance, *Phys. Rev. E* **108**, 034106 (2023).

[26] Y. Khedif, S. Haddadi, M. Daoud, H. Dolatkhah, and M. R. Pourkarimi, Non-classical correlations in a Heisenberg spin model with Heitler–London approach, *Quantum Information Processing* **21**, 235 (2022).

[27] M. Hashem, A.-B. A. Mohamed, S. Haddadi, Y. Khedif, M. R. Pourkarimi, and M. Daoud, Bell nonlocality, entanglement, and entropic uncertainty in a Heisenberg model under intrinsic decoherence: DM and KSEA interplay effects, *Applied Physics B* **128**, 87 (2022).

[28] A. Ali, S. Al-Kuwari, and S. Haddadi, Trade-off relations of quantum resource theory in Heisenberg models, *Physica Scripta* **99**, 055111 (2024).

[29] C. J. van Diepen, T.-K. Hsiao, U. Mukhopadhyay, C. Reichl, W. Wegscheider, and L. M. Vandersypen, Quantum simulation of antiferromagnetic Heisenberg chain with gate-defined quantum dots, *Physical Review X* **11**, 041025 (2021).

[30] P. Cappellaro, C. Ramanathan, and D. G. Cory, Simulations of information transport in spin chains, *Physical Review Letters* **99**, 250506 (2007).

[31] F. Meier, J. Levy, and D. Loss, Quantum computing with spin cluster qubits, *Physical Review Letters* **90**, 047901 (2003).

[32] H. Yu, Y. Zhao, T.-C. Wei, *et al.*, Simulating large-size quantum spin chains on cloud-based superconducting quantum computers, *Physical Review Research* **5**, 013183 (2023).

[33] R. Liu, Y. Chen, M. Jiang, X. Yang, Z. Wu, Y. Li, H. Yuan, X. Peng, and J. Du, Experimental critical quantum metrology with the Heisenberg scaling, *npj Quantum Information* **7**, 170 (2021).

[34] M. M. Rams, P. Sierant, O. Dutta, P. Horodecki, and J. Zakrzewski, At the limits of criticality-based quantum metrology: Apparent super-Heisenberg scaling revisited, *Physical Review X* **8**, 021022 (2018).

[35] F. Ozaydin and A. A. Altintas, Quantum metrology: Surpassing the shot-noise limit with Dzyaloshinskii–Moriya interaction, *Scientific Reports* **5**, 16360 (2015).

[36] R. T. Chepuri and I. A. Kovács, Complex quantum network models from spin clusters, *Communications Physics* **6**, 271 (2023).

[37] S. Abaach, Z. Mzaouali, and M. El Baz, Long distance entanglement and high-dimensional quantum teleportation in the fermi–hubbard model, *Scientific Reports* **13**, 964 (2023).

[38] F. Benabdallah, S. Haddadi, H. Arian Zad, M. R. Pourkarimi, M. Daoud, and N. Ananikian, Pairwise quantum criteria and teleportation in a spin square complex, *Scientific Reports* **12**, 6406 (2022).

[39] I. Dzyaloshinsky, A thermodynamic theory of “weak” ferromagnetism of antiferromagnetics, *Journal of physics and chemistry of solids* **4**, 241 (1958).

[40] I. Dzialoshinskii, Thermodynamic theory of weak ferromagnetism in antiferromagnetic substances, *Soviet Physics JETP-USSR* **5**, 1259 (1957).

[41] A. Fert, M. Chshiev, A. Thiaville, and H. Yang, From early theories of Dzyaloshinskii–Moriya interactions in metallic systems to today’s novel roads, *Journal of the Physical Society of Japan* **92**, 081001 (2023).

[42] T. Moriya, Anisotropic superexchange interaction and weak ferromagnetism, *Physical Review* **120**, 91 (1960).

[43] L. Shekhtman, A. Aharony, and O. Entin-Wohlman, Bond-dependent symmetric and antisymmetric superexchange interactions in La_2CuO_4 , *Physical Review B* **47**, 174 (1993).

[44] T. Yildirim, A. B. Harris, A. Aharony, and O. Entin-Wohlman, Anisotropic spin Hamiltonians due to spin-orbit and Coulomb exchange interactions, *Physical Review B* **52**, 10239 (1995).

[45] T. E. Lee, S. Gopalakrishnan, and M. D. Lukin, Unconventional magnetism via optical pumping of interacting spin systems, *Physical Review Letters* **110**, 257204 (2013).

[46] A. Signoles, T. Franz, R. F. Alves, M. Gärttner, S. Whitlock, G. Zürn, and M. Weidemüller, Glassy dynamics in a disordered Heisenberg quantum spin system, *Physical Review X* **11**, 011011 (2021).

[47] P. Scholl, H. J. Williams, G. Bornet, F. Wallner, D. Barredo, L. Henriet, A. Signoles, C. Hainaut, T. Franz, S. Geier, *et al.*, Microwave engineering of programmable XXZ Hamiltonians in arrays of Rydberg atoms, *PRX Quantum* **3**, 020303 (2022).

[48] J. Gaudet, E. Smith, J. Dudemaine, J. Beare, C. Buhariwalla, N. Butch, M. Stone, A. Kolesnikov, G. Xu, D. Yahne, *et al.*, Quantum spin ice dynamics in the dipole-octupole pyrochlore magnet $\text{Ce}_2\text{Zr}_2\text{O}_7$, *Physical Review Letters* **122**, 187201 (2019).

[49] A. S. Patri, M. Hosoi, and Y. B. Kim, Distinguishing dipolar and octupolar quantum spin ices using contrasting magnetostriction signatures, *Physical Review Research* **2**, 023253 (2020).

[50] G. Chen, Coulombic antiferromagnet in spin-1/2 pyrochlores with dipole-octupole doublets, *Physical Review*

Research **5**, L032027 (2023).

[51] P. Rosenberg and E. Manousakis, Quantum Weyl–Heisenberg antiferromagnet, Physical Review B **108**, 214431 (2023).

[52] F. Fanchini, T. Werlang, C. Brasil, L. Arruda, and A. Caldeira, Non-Markovian dynamics of quantum discord, Physical Review A **81**, 052107 (2010).

[53] W. K. Wootters, Entanglement of formation and concurrence., Quantum Inf. Comput. **1**, 27 (2001).

[54] C. Branciard, E. G. Cavalcanti, S. P. Walborn, V. Scarani, and H. M. Wiseman, One-sided device-independent quantum key distribution: Security, feasibility, and the connection with steering, Physical Review A **85**, 010301 (2012).

[55] Q. He, L. Rosales-Zárate, G. Adesso, and M. D. Reid, Secure continuous variable teleportation and Einstein–Podolsky–Rosen steering, Physical Review Letters **115**, 180502 (2015).

[56] Y. Z. Law, J.-D. Bancal, V. Scarani, *et al.*, Quantum randomness extraction for various levels of characterization of the devices, Journal of Physics A: Mathematical and Theoretical **47**, 424028 (2014).

[57] M. Piani and J. Watrous, Necessary and sufficient quantum information characterization of Einstein–Podolsky–Rosen steering, Physical Review Letters **114**, 060404 (2015).

[58] E. G. Cavalcanti, S. J. Jones, H. M. Wiseman, and M. D. Reid, Experimental criteria for steering and the Einstein–Podolsky–Rosen paradox, Physical Review A **80**, 032112 (2009).

[59] A. Costa and R. Angelo, Quantification of Einstein–Podolsky–Rosen steering for two-qubit states, Physical Review A **93**, 020103 (2016).

[60] K. Bartkiewicz, B. Horst, K. Lemr, and A. Miranowicz, Entanglement estimation from Bell inequality violation, Physical Review A **88**, 052105 (2013).

[61] K. Bartkiewicz, K. Lemr, A. Ćernoch, and A. Miranowicz, Bell nonlocality and fully entangled fraction measured in an entanglement-swapping device without quantum state tomography, Physical Review A **95**, 030102 (2017).

[62] R. Horodecki, P. Horodecki, and M. Horodecki, Violating Bell inequality by mixed spin-1/2 states: necessary and sufficient condition, Physics Letters A **200**, 340 (1995).

[63] W.-Y. Sun, D. Wang, and L. Ye, How relativistic motion affects Einstein–Podolsky–Rosen steering, Laser Physics Letters **14**, 095205 (2017).

[64] M.-L. Hu, Relations between entanglement, Bell-inequality violation and teleportation fidelity for the two-qubit X states, Quantum information processing **12**, 229 (2013).

[65] M. A. Yurishev, On the quantum correlations in two-qubit XYZ spin chains with Dzyaloshinsky–Moriya and Kaplan–Shekhtman–Entin–Wohlm–Aharony interactions, Quantum Inf. Process. **19**, 336 (2020).

[66] M. A. Yurishev and S. Haddadi, Local quantum Fisher information and local quantum uncertainty for general X states, Phys. Lett. A **476**, 128868 (2023).

[67] Y. Khedif, S. Haddadi, M. R. Pourkarimi, and M. Daoud, Thermal correlations and entropic uncertainty in a two-spin system under DM and KSEA interactions, Modern Physics Letters A **36**, 2150209 (2021).

[68] E. I. Kuznetsova, M. A. Yurishev, and S. Haddadi, Quantum Otto heat engines on XYZ spin working medium with DM and KSEA interactions: operating modes and efficiency at maximal work output, Quantum Information Processing **22**, 192 (2023).